 https://doi.org/10.24191/jeesr.v20i1.016

Robot Arm Imitating Human Upper Arm: The Design and Stress Analysis

M.S.I.M Sabari and R.L.A. Shauri*

***Abstract*—In previous work, a developed four degree of freedom (DoF) arm failed to move in actual experiment due to the vibration that occurred at the first joint which carries the heaviest payload of the arm. It indicates the importance of analysing robot design before a prototype can be built for real motion. A new robotic arm that was designed to imitate a human upper arm has four joints which rotate around x, y, and z-axis to move its four links to the required posture of the wrist. The work demonstrates the use of a design software to confirms feasibility of the joints for motion and finite element analysis (FEA) to predict the behaviour of the structure when under force. FEA results showed that most of the links have experienced lower stress levels than of the tensile yield strength of alloy steel material which proved the strength of the structure to sustain the applied 15Nm stress test. Hence, with minor adjustments to match with the size of the existing robot hand, the design is ready for fabrication process in the next study.**

***Index Terms*—3D mechanical design, geometric structure, human upper arm, finite element analysis, robot arm.**

I. Introduction

ROBOTS have been developed based on science, mathematics and technology to help human in dirty, repetitive, dangerous and impossible tasks. They are made of mechanical hardware and electronics that are being produced for various purpose and applications, not limited to the industrial area only. They become the favourable option in the situations when humans are unable to deal with dangerous, dirty and long duration tasks.

Robots which are designed with the imitation of human features are normally expected to carry out more delicate and difficult tasks. For example, robotic arms are capable of moving an object from one place to another by replicating how human doing it. Moreover, they can carry the job precisely with an object which is much heavier or very small in size, which may be impossible for human worker to do it.

Robotic arm is made up by using different solid parts such as direct shaft, high torque motor, links, joints and connectors, where an n-th number of joints that a robot arm has will produce an n-th degree of freedom (DoF) of the robot. The structure type can be divided to Cartesian, articulated, spherical and parallel, which can be arranged by researchers to control the motion of their robotic arm [1]. Via the assistance of a controller, a robotic arm can control its joint variables according to the values desired by the user. There are basically seven DOF in a human arm, but for robotic arms, reducing this to six or less can make them imitate specific working skills of human [2].

A 4-DoF climbing robot was designed with high manoeuvrability using inverse kinematics calculations where the model was fabricated for trial operations. It has high manoeuvrability as climbing robot by imitating the physical structure of an insect. To create the capability of climbing rough surfaces, claw inspired robot (CLIBO) structure was designed with some rock-climbing techniques. The robot is made up of four legs that are symmetrically placed around the robot's central body and moved according to the proposed motion algorithm [3].

In solving the issues faced by existing wearable rehabilitation devices, an upper limb exoskeleton rehabilitation robot was designed to be flexible, portable, lightweight, high accuracy performance and easy to wear [4]. The 3-DoF joints consist of one for the elbow and two for the wrist. They were mostly adjustable to change the device size, thus allowing the patients to wear it comfortably. The design of a 3-DoF arm based on FreeCAD in [5] was used to visualize the movement and sensor measurements over robot operating system (ROS) interface. The robot was instructed for a pick-and-place using position control and switchable to use force control for lifting up the grasped object. Meanwhile, a 4-DoF robot arm was built to swing racket-head with high speed using its humanoid arm structure powered by pneumatic actuators [6]. The robot is directed to follow the trajectory provided by geometric requirements to obtain the faster speed than achieved by previous robotic arms. Accuracy of the pneumatic motor position is confirmed by applying feedback control to the system.

A neurorehabilitation robot named NeReBot was built to assist post stroke patient [7]. The patient's upper limbs are connected to wires that are adjustable in length and pulled by electric motors. The required motions of patient upper limb are designed according to the specialized trajectory by rehabilitation therapist. Author claimed that the NeReBot is

This manuscript is submitted on 2nd November 2021 and accepted on 28th Feb 2022. This work was supported Malaysia Ministry of Higher Education (MOHE) under Grant FRGS (600-IRMI/FRGS 5/3 (326/2019)".

M.S.I.M Sabari was a student in the School of Electrical Engineering, College of Engineering, Universiti Teknologi MARA, 40450 Shah Alam, Malaysia. He is now working as a production engineer with BESI APAC Sdn Bhd, Malaysia (e-mail: shazreensabari@gmail.com).

R. L. A. Shauri is a senior lecturer with the School of Electrical Engineering, College of Engineering, Universiti Teknologi MARA, 40450 Shah Alam, Malaysia (e-mail: ruhizan@uitm.edu.my).

*Corresponding author
Email address: ruhizan@uitm.edu.my

more cost effective, provide safer treatment, highly acceptable by patients and transportable to any location of the patient inside the hospital. Human arm is also used to move a master-slave exoskeleton arm robot [8]. They proposed an adaptive coordination control based on the human impedance profiles extracted from the master or human assisted arm to the slave arm robot in [9]. The measured surface EMG signals from the muscles were converted to human stiffness and used by the controller to produce the reference trajectory.

On the other hand, a different type of manipulator robot was modelled to be placed on an unmanned aerial vehicle called ASCTEC PELICAN [10]. The 5-DoF arm called PUL5AR was carefully designed to be light-weight due to the weight constraints from the limited payloads and energy consumption. Furthermore, the centre of gravity of the arm needs to be the closest possible to the body of the UAV to secure the balance during operation [11].

Finite element method (FEM) is a method that researchers have been using to predict the failure of an object structure or material when an amount of stress is applied onto the design. The resulted analysis helps them to understand the behaviour of the structure without the need of the physical prototype. Finite element analysis (FEA) has been used by [12] to confirm the design of a 4-DoF desktop stacking arm manipulator. Joint stress results were significantly lower than the yield stress of the chosen no. 45 steel material, thus proven that the critical stressed parts of the arm show sufficient strength and stiffness which satisfies the requirements for the robot's application.

A new magnetic flux leakage (MFL) sensor design was proposed for pipeline inspection gauge carried by a self-driving robot [13]. The design was verified through simulation by FEA and also experimentally to prove its capability of reducing magnetic force signal during robot's movement through the pipeline while increasing the detection sensitivity of the defects.

Conventional flexible microactuators (FMA) used for robotic mechanism are normally reinforced with fibers to produce the elasticity for deformation or bending of the structure. The complicated fabrication process is what caused the FMA to be expensive. Therefore, a new nonreinforced (FMA) design is developed using sensitivity analysis of nonlinear hyperelastic finite-element-method (FEM) [14]. The bending angle, radial expansion ratio and maximum stress on the wall of the FMA were analysed by FEM to obtain the optimized characteristics of the fibreless FMA.

A modular sweeping robot namely hTerto was developed consisting of four rectangular blocks connected via passive hinges and steered by differential drive from two wheels [15]. Improvements made to the previous design include replacing the brush type and increasing the vacuum bin's size. Finite element analysis of the cleaning module was implemented to observe the structural deformations, natural frequencies and stress patterns of the bristle and the rolling brush under static loading. From the analysis results, authors observed very small maximum stress on the brush compared to the yield strength value of the ABS material which confirms the absence of deformation, hence the safe use of the design. The deformations patterns of the bristles with selected materials provide useful information on the efficiency of sweeping action of the brush.

The above studies prove that FEA simulation is an informative and reliable method that can be used by researchers to anticipate the strength of a design structure in terms of its durability and stress limit under some applied stress. It indicates the importance of analysing any design of robots before a prototype can be built for real motion.

Learning from previous experience where a developed four degree of freedom (DoF) arm failed to move due to weak connection of the joints, analyzing a new arm design to observe the strength of the structure beforehand is vital. Thus, this paper presents a new design of a 4-DoF arm that imitates the upper arm of human for manipulating light object. The work demonstrates the use of a design software to confirms feasibility of the joints for motion and FEA analysis to predict the behaviour of the structure when under force. FEA is used to simulate the structure under an amount of applied force i.e. the gravity force that pulls the links and joints downwards/inwards which is similar to the situation when the arm needs to carry loads during motion. The identified weak points will give good information for the arm's operation and payload limits to avoid damaging the arm parts during real implementation in the future.

II. Robot Design

A. Robot structure

In this work, a new design of a 4-DoF arm is proposed for manipulating light object application. The design is required to rotate around xyz-axis to gain wide range of working space for robotics assignments like grasping and pick-and-place task. The structure was decided based on the required application of the robot arm. In this case, the robot needs to imitate the structure of a human upper arm as shown in Fig. 1a while not exceeding four DoF to maintain simplicity for position control in the future. The four degree of freedom feature is indicated by the four rotatable joints that rotate around specified axes directions.

There are four joints in this structure, where joint 1 2, 3 and 4 are labeled as P, Q, R, and S, respectively. Joint 1 until joint 4 are revolute joint types with axis rotation as written in Table I. Motor shafts are connected directly to each link to produce the rotary motions around the axis, in the range of the degrees as specified in the same table. The first joint is the twisting joint (T type), joint 2 is revolving joint (type V), joint 3 is twisting joint (T type) and the joint 4 is revolving joint (type V).

As shown in Fig. 1b, joint 1 (located inside the upper part of the vertical pole of the robot's base) is directly driven by motor M1, joint 2 (the robot's shoulder) is driven by motor M2, joint 3 is driven by motor M3 which is placed inside link 2 and finally joint 4 is driven by motor M4 to move link 4 like human elbow.

The link starts from the origin point A followed by PQ, QR, RS and ST links. These links connect the segments between each joint P, Q, R, and S to construct the shoulder-to-elbow structure of an arm while T is the point at the robot's wrist before an end effector of the required application can be attached. B, C, D, and E are the centres of gravity of the respective links and will be useful for kinematics calculations.

All four links are arranged in serial and actuated by the respective joint 1 to 4.

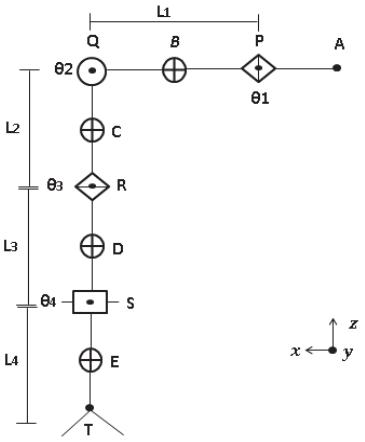

a) Skeleton diagram of human upper arm

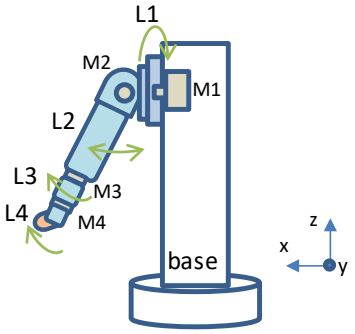

b) Illustation of the robot's links and joints composed together to imitate a human upper arm

Fig. 1. Structure of the proposed 4-DoF robot arm

TABLE I
ROTATION RANGE AND DIRECTION OF EACH JOINT OF THE PROPOSED ROBOT

Joint	Rotation from initial condition	Rotation around
1	-180˚ to 180˚	x-axis
2	-90˚ to 45˚	y-axis
3	-150˚ to 150˚	z-axis
4	-90˚ to 90˚	x-axis

B. Design Using SolidWorks

The 3D mechanical designs of the joints and links were drawn with suitable shapes and dimensions in order to make sure that all components match and fit with each other.

The first important step is to set the coordinate axis as the base reference of the drawing. This is to make sure that the joints and links are drawn to provide the desired rotation. The dimension of each part needs to consider the dimensions of the on-the-shelf components like the gears and motors to avoid any misalignment issue when fixing those components in the fabricated design in the future.

Figure 2 shows the SolidWorks drawing plane for sketching the robot components. Two steps are involved which consist of the component's design and assembly as shown by the selections in Fig. 3. First, the "Part" section is selected to sketch the 3D component of the first joint of the robot arm. This step is repeated to create all components of the first joint with the proposed mechanism which requires the linkage, gears, motor and shaft. The process repeats also for the other joints. Once all components are created, the mate process is the next step to do by selecting the "Assembly" section where in this step the components will be assembled as one body of the robot arm.

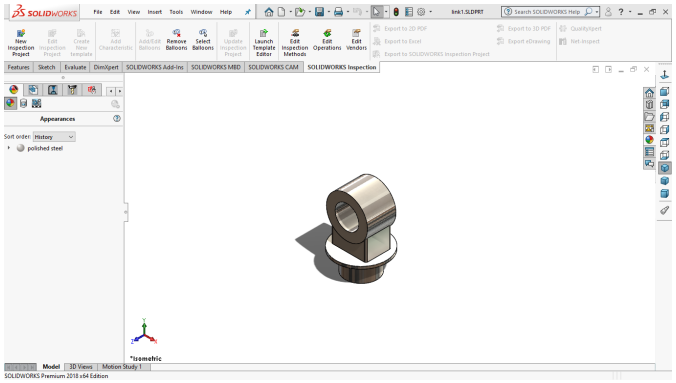

Fig. 2. Drawing canvas to draw each arm's part in Solidworks software

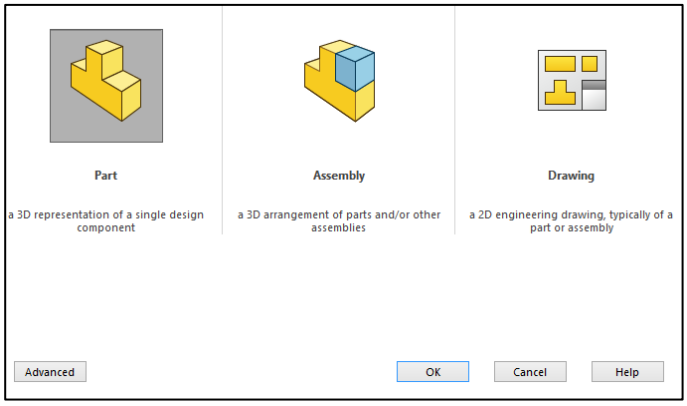

Fig. 3. Each Arm's Part will be Drawn using Part Section while Assembly Section is to Assemble the Designed Components

Simulation for motion of the assembled body can also be performed in the assembly section. This can be done by directly clicking and rotating the links in the directions of x, y or z-axis. In the case where the link does not fulfil the required movement, the design of the related part/parts need to be revised and drawn. Once the simulation is satisfied, the arm's design is ready to be tested for strength.

Figure 4 shows the design of the four links of the proposed robot design. The curves and holes of the parts were designed based on specific dimensions to make sure that all links are connected to the joints and conform to the specified direction of the rotation in Table I.

Next, the simulation of the assembled robot design is implemented for several rotation angles as tabulated in Table II. Conditions 1 until 4 were tested for individual joints while the fifth condition was tested when all joints are rotated at the same time. The zero position or the standby position of the robotic arm is shown in Fig. 5(a). By rotating the links in the SolidWorks, the arm moved smoothly according to the different conditions as can be observed in Figs. 5(b)-(f). This proved that the dimensions between the components are in line with each other to produce the arm movement.

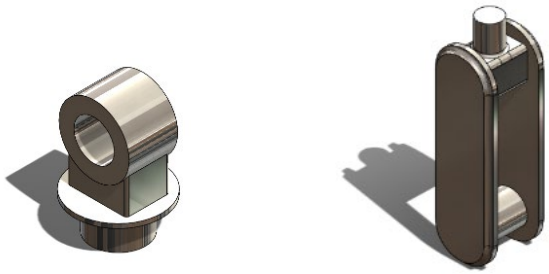

a) Link 1 b) Link 2

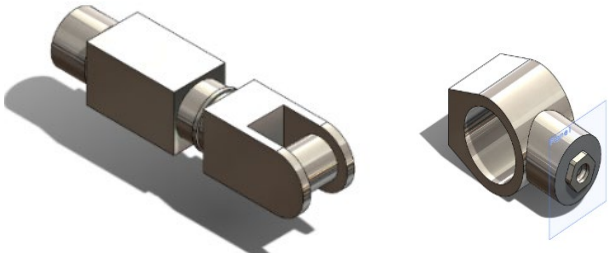

c) Link 3 d) Link 4

Fig. 4. The Created 3D Drawings of the Four Links of the Robot Arm

TABLE II
ROTATION TESTS APPLIED TO THE ASSEMBELD BODY TO CHECK MOTION OF EACH LINK

Condition	Assigned link	Rotation from initial condition
1	Link 1	180˚
2	Link 2	-45˚
3	Link 3	45˚
4	Link 4	90˚
5	All links	Random theta

a) Robot arm at initial condition b) Link 1 at Condition 1

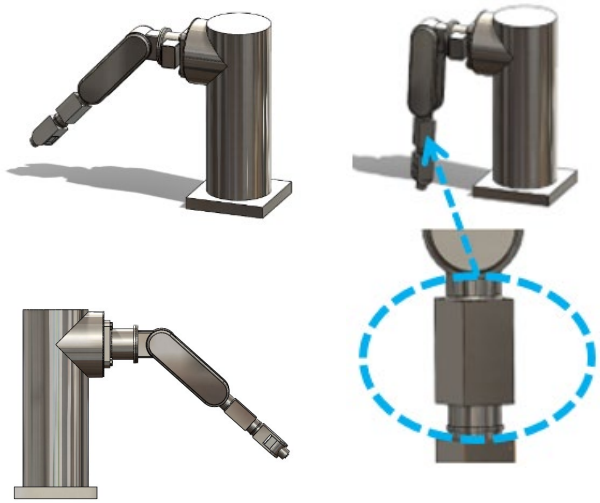

c) Link 2 at Condition 2 d) Link 3 at Condition 3

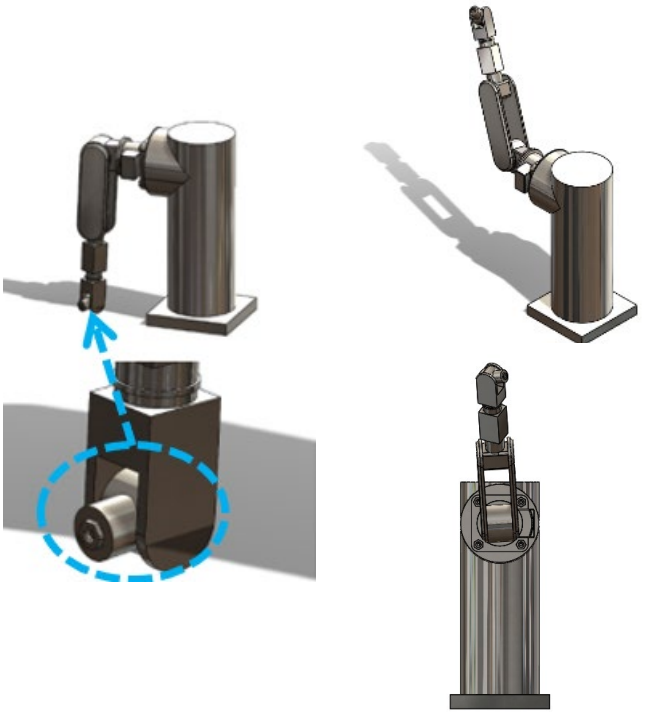

e) Link 4 at Condition 4 f) Robot arm at Condition 5

Fig. 5. Simulation Results of Joint Rotation Test according to Five Conditions in Table II

C. *Finite Element Analysis Using SolidWorks*

In this step, the proposed design in tested for torque analysis using finite element analsyis (FEA) method to ensure the strength of the link design with the proposed material under a specific value of applied torque. This simulation is performed on the SolidWorks drawings of the links' components.

The presetting window for the simulation are shown in Fig. 6 and Fig. 7 where the value of the applied torque is set to 15Nm and the material for the design was chosen as alloy steel. Here, von-Mises stress which commonly used on ductile materials is selected as the failure criterion to indicate whether the design with the selected material could sustain or fracture under the applied torque. As long as the measurement of the yield is lower than the von-Mises stress of the alloy steel value i.e. 620.422MPa from Fig. 6, the design can be accepted. The simulation torque is applied around the rotation axis of the joints of each link as shown in Fig. 8(a). For example, in SolidWorks, the direction of the applied torque on link 2 is indicated by the small arrow around the pink coloured cylindrical part as the centre of rotation shown in Fig. 8(b). The surface of the robot part where the torque is applied is shown in blue colour in the same figure.

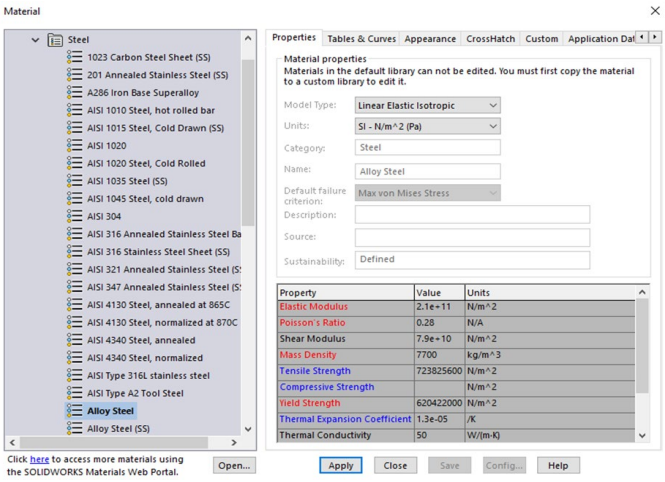

Fig. 6. Setting the Design Material as Alloy Steel before Running FEA

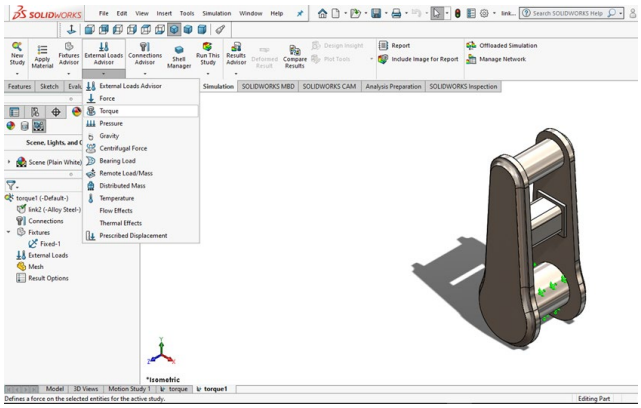

Fig. 7. Setting Torque Amount and Direction using External Panel Advisor

The following figures show the results of the von-Mises stress simulation. The thermal colours represent the value of the stress level applied by the links against the tension given by the 15 Nm torque. The lowest stress level is blue, followed by green, yellow, and finally red, with red being the highest. It can be observed from Fig. 9(a) that link 1 experienced the stress levels in the range of 4.527×10^5 to 8.350×10^5 Pa which is still lower than the tensile yield strength of the alloy steel 6.20422×10^8 Pa, as indicated by the small red coloured arrow in the coloured von Mises incdexfigure. Similarly, link 2 and link 3 also experienced the stress levels within the tensile yield strength value which means that the proposed design can withstand the tension applied to the body of the links. It is important for the upper links especially link 1 to sustain the applied force since they will have to carry heavier payload that includes the lower links.

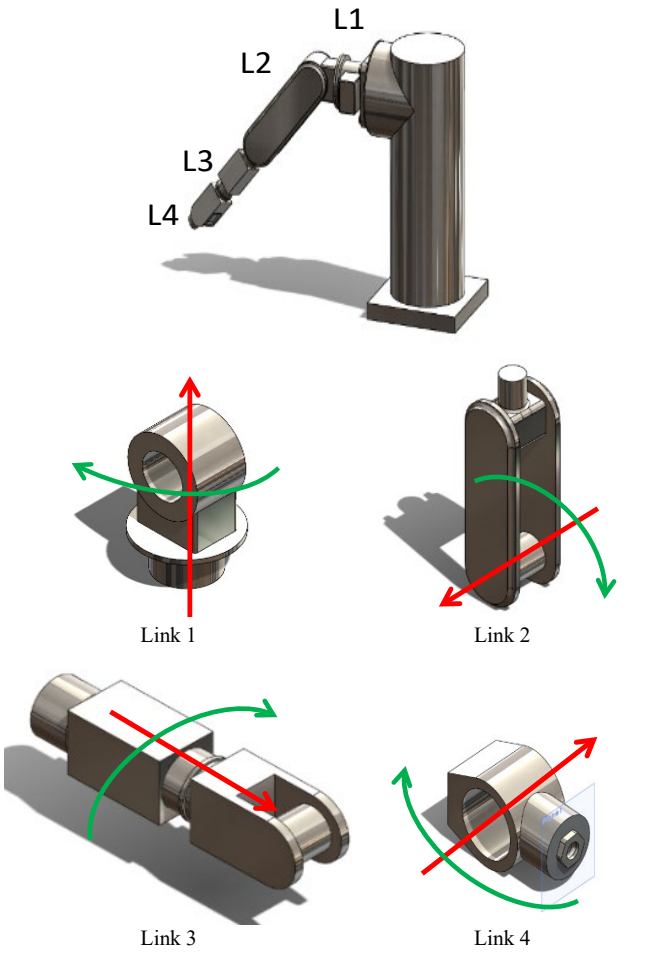

a) llustration of Rotations and Axes Directions of the Applied Torque for FEA

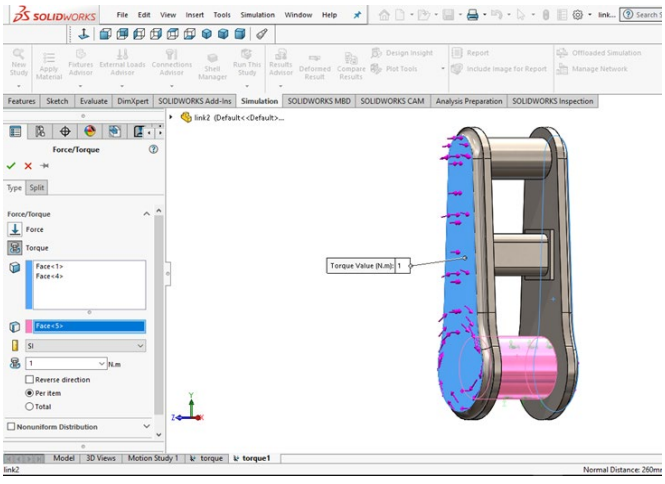

b) Example for link 2

Fig. 8. Setting Up the Rotation Axis and Force Direction of Applied Torque for Each Component in SolidWorks

Consequently, higher stress level can be observed for the simulation result on link 4 as shown in Fig. 9(d). This is due to the higher impact of the applied 15N force to link 4 which comparatively smaller than the other links. In fact, since the link is the farthest from the shoulder base, it will carry the payload from the end effector and the object to be manipulated only. Thus, redesign depends on the size of end effector and the type of task that will be assigned later.

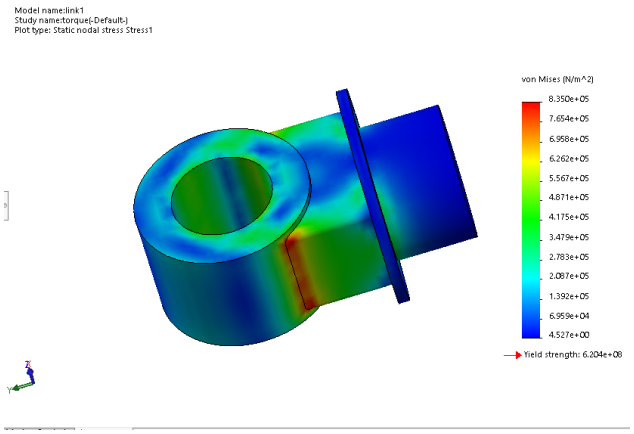

a) Link 1

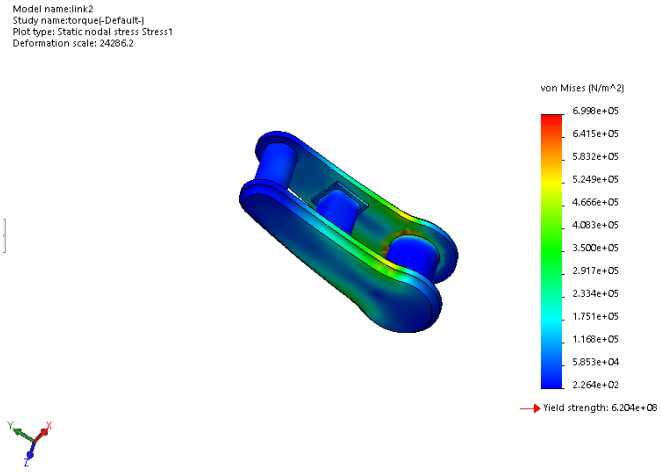

b) Link 2

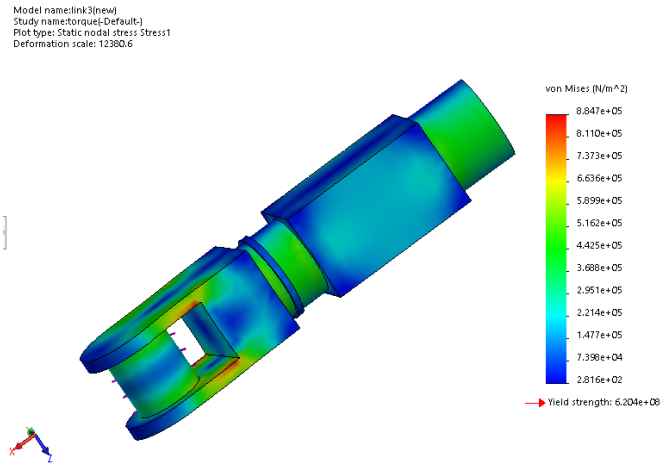

c) Link 3

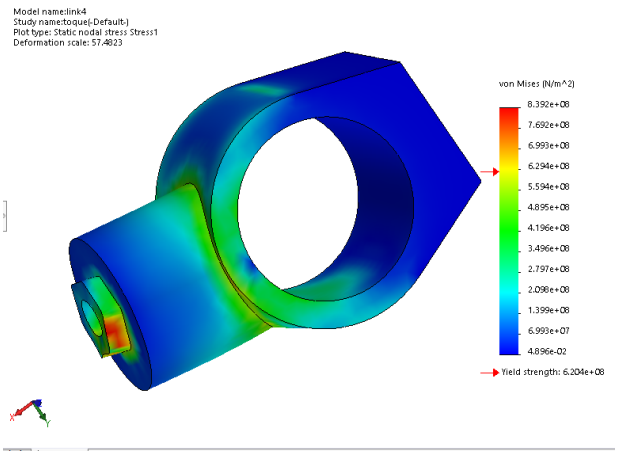

d) Link 4

Fig. 9. FEA Simulation Results for All Four Link according to the Applied Torque

III. Conclusion

This paper presents the design of a 4-DoF arm that imitates upper arm of human for light object manipulaton. The total number, types of rotation and dimension of the joints and links have been carefully selected and drawn. From the simulation results, link 1, link 2 and link 3 have been found to be able to withstand the tension of 15N which is equivalent to about 1.5kg of weight applied to the body of each link. This fulfilled the design requirement where the upper links especially link 1 need to be able to sustain the applied force well as they will have to carry heavier payload which includes their lower links. On the other hand, slightly higher stress level was obtained for link 4 which was due to the higher impact of the applied 15N force to the comparatively smaller area of the link. This is not critical since link 4 is the farthest from the shoulder base and will carry the payload from the end effector and the object to be manipulated only which can be limited to less than the equivalent 1.5kg. However, redesigning of link 4 may be required depending on the weight of the payloads in the assigned task in future work.

Acknowledgment

This research is supported by FRGS (600-IRMI/FRGS 5/3 (326/2019) grant. The authors acknowledged Malaysia Ministry of Higher Education (MOHE) for the approved fund and to College of Engineering, Universiti Teknologi MARA for providing the laboratory space and equipments.

References

[1] N. Sarkar, X. Yun, and V. Kumar, "Dynamic control of 3-D rolling contacts in two-arm manipulation," *IEEE Transactions on Robotics and Automation*, vol. 13, no. 3, pp. 364–376, 1997.

[2] D. J. Gonzalez and H. H. Asada, "Triple Scissor Extender: A 6-DoF lifting and positioning robot," in *Proc. IEEE Int. Conf. Robot. Autom.*, vol. 2016-June, pp. 847–853, 2016.

[3] S. Parvathi and S. T. Selvi, "Design and fabrication of a 4 Degree of Freedom (DOF) robot arm for coconut harvesting," in *Proc. 2017 International Conference on Intelligent Computing and Control (I2C2)*, 2017, pp. 1-5.

[4] B. Gao, H. Ma, S. Guo, H. Xu, and S. Yang, "Design and evaluation of a 3-degree-of-freedom upper limb rehabilitation exoskeleton robot," in *Proc. 2017 IEEE Int. Conf. Mechatronics Autom. ICMA*, 2017, pp. 938–942.

[5] S. Hernandez-Mendez, C. Maldonado-Mendez, A. Marin-Hernandez, H. V. Rios-Figueroa, H. Vazquez-Leal, and E. R. Palacios-Hernandez, "Design and implementation of a robotic arm using ROS and MoveIt!," in *Proc. 2017 IEEE International Autumn Meeting on Power, Electronics and Computing* (ROPEC), 2017.

[6] S. Mori, K. Tanaka, S. Nishikawa, R. Niiyama and Y. Kuniyoshi, "High-Speed and Lightweight Humanoid Robot Arm for a Skillful Badminton Robot," *IEEE Robotics and Automation Letters*, vol. 3, no. 3, pp. 1727-1734, July 2018.

[7] G. Rosati, P. Gallina, and S. Masiero, "Design, implementation and clinical tests of a wire-based robot for neurorehabilitation," *IEEE Trans. Neural Syst. Rehabil. Eng.*, vol. 15, no. 4, pp. 560–569, 2007.

[8] A. Ajoudani, C. Fang, N. G. Tsagarakis, and A. Bicchi, "A reduced complexity description of arm endpoint stiffness with applications to teleimpedance control," in *Proc. IEEE/RSJ Int. Conf. Intell. Robots Syst. (IROS)*, Hamburg, Germany, 2015, pp. 1017–1023.

[9] B. Huang, Z. Li, X. Wu, A. Ajoudani, A. Bicchi, and J. Liu, "Coordination Control of a Dual-Arm Exoskeleton Robot Using Human Impedance Transfer Skills," *IEEE Trans. Syst. Man, Cybern. Syst.*, vol. 49, no. 5, pp. 954–963, 2019.

[10] Ascending technologies, gmbh. [Online]. Available: http://www.asctec.de/.

[11] C. D. Bellicoso, L. R. Buonocore, V. Lippiello, and B. Siciliano, "Design, modeling and control of a 5-DoF light-weight robot arm for aerial manipulation," in *Proc. 2015 23rd Mediterranean Conference on Control and Automation (MED)*, 2015, pp. 853-858.

[12] RobotWorx. 2019. What Are The Main Types Of Robots?. [online] Available at: <https://www.robots.com/faq/what-are-the-main-types-of-robots> [Accessed 5 June 2020].